



# Distribution, stock, and influencing factors of soil organic carbon in an alpine meadow in the hinterland of the Qinghai–Tibetan Plateau

XUCHAO ZHU<sup>1,2</sup> and MING'AN SHAO<sup>1,3,\*</sup>

<sup>1</sup>Key Laboratory of Ecosystem Network Observation and Modeling, Institute of Geographic Sciences and Natural Resources Research, Chinese Academy of Sciences, Beijing 100 101, China.

<sup>2</sup>State Key Laboratory of Soil and Sustainable Agriculture, Institute of Soil Science, Chinese Academy of Sciences, Nanjing 210 008, China.

<sup>3</sup>College of Resources and Environment, University of Chinese Academy of Sciences, Beijing 100 190, China.

\*Corresponding author. e-mail: shaoma@igsrr.ac.cn

MS received 22 February 2017; revised 3 September 2017; accepted 8 November 2017;  
published online 30 June 2018

Understanding the spatial distribution, stocks, and influencing factors of soil organic carbon (SOC) is important for understanding the current situation of SOC in alpine meadow ecosystems on the Qinghai–Tibetan Plateau (QTP). We sampled 23 soil profiles to a depth of 50 cm in a 33.5 hm<sup>2</sup> plot in a typical meadow on the central QTP. The distribution, stock and influencing factors of SOC was then analyzed. The mean density of soil carbon content (SOC<sub>D</sub>) was 2.28 kg m<sup>-2</sup> with a range of 5.99 kg m<sup>-2</sup>. SOC<sub>D</sub> in the 0–10 cm layer was 3.94 kg m<sup>-2</sup> and decreased quadratically with depth. The total stock of SOC to a depth of 50 cm was ca. 2950 t, the 0–10 and 0–30 cm layers accounting for 38 and 80%, respectively. SOC<sub>D</sub> varied moderately spatially and was distributed more homogeneously in the 0–10 and 40–50 cm layers but was more variable in the middle three layers. SOC<sub>D</sub> was significantly correlated positively with soil-water content, total porosity, and silt content and negatively with soil pH, bulk density, stone content and sand content. This study provides an important contribution to understanding the role of alpine meadows in the global carbon cycle. It also provides field data for model simulation and the management of alpine meadow ecosystems.

**Keywords.** Soil organic carbon; spatial distribution; influencing factors; alpine meadow; Qinghai–Tibetan Plateau.

## 1. Introduction

Soil organic carbon (SOC) is an important component of soil and can influence the stability and development of natural ecosystems by influencing soil structure, fertility, and water holding capacity (Liu *et al.* 2011). Soil contains the largest pool of SOC of terrestrial ecosystems, twice the total content of the atmosphere and biosphere (Yang

*et al.* 2008; Zhang and Shao 2014). SOC stock fluctuates with changes of land use, tillage strategies, soil erosion, and grassland degradation, which can influence not only the physical, chemical, and biological properties of soil, but also local even global carbon cycles (Li and Shao 2014).

The distribution (Yu *et al.* 2007; Zhang and Shao 2014; Bameri *et al.* 2015), stock estimation (Fu *et al.* 2010; Yang *et al.* 2016), influencing factors

(Li and Shao 2014; Zhao *et al.* 2015), and model simulation (Meersmans *et al.* 2009a; Koszinski *et al.* 2015; Yang *et al.* 2016) of SOC have been studied widely in recent decades on global (Batjes 1996), national (Ottoy *et al.* 2015; Roßkopf *et al.* 2015; Zhang *et al.* 2015a; Aitkenhead and Coull 2016; Mulder *et al.* 2016; Rodríguez Martín *et al.* 2016; Wen and He 2016), regional (Liu *et al.* 2011; Wang *et al.* 2015b), and watershed (Wei *et al.* 2010; Xin *et al.* 2016) scales in forests (Wei *et al.* 2010; Ricker and Lockaby 2015), grasslands (Shi *et al.* 2012; Zhao *et al.* 2015), croplands (Wang *et al.* 2015a), wetlands (Li and Shao 2014), and deserts (Zhang and Shao 2014) on plains (Koszinski *et al.* 2015), mountains (Chen *et al.* 2016), hills (Bameri *et al.* 2015; Xin *et al.* 2016), and plateaus (Wang *et al.* 2015b; Zhao *et al.* 2015).

The Tibetan Plateau is the highest unit of physical geography in the world (Zhang *et al.* 2015c) and has been called the third pole of the Earth (Qiu 2008). It functions as an important barrier for the ecological security of China and even for all Asia and is an important indicator of global climate change (Sun *et al.* 2012). Alpine meadows are widely distributed across the plateau and cover a total area of 0.7 million km<sup>2</sup>. However, the local ecosystems developed in this high, cold, and oxygen-deficit environment, are fragile and degenerating due to climate change and over-grazing in recent decades (Li and Shao 2014). The degradation of the ecosystem has reduced land productivity and species diversity and changed the soil-water status (Li *et al.* 2014; He and Richards 2015; Li *et al.* 2016). The study of SOC, an important component of the soil, is thus necessary and has received some attention on the Qinghai–Tibetan Plateau (QTP) (Wang *et al.* 2002; Yang *et al.* 2008; Baumann *et al.* 2009; Tan *et al.* 2010; Chen *et al.* 2016; Yang *et al.* 2016). Yang *et al.* (2008) estimated the SOC stock of the QTP based on 405 soil profiles and the enhanced vegetation index from satellite data and analyzed the relationship between SOC with climatic factors and soil textures. Baumann *et al.* (2009) analyzed the influence of frozen earth on SOC stocks from 47 soil profiles on a 1200 km transect on the QTP. Tan *et al.* (2010) estimated the biomass and SOC stock of grassland on the QTP using the ORCHIDEE global vegetation model. Studies of SOC on the QTP have mainly concentrated on large-scale inversion and estimation, which have low or uncertain accuracies due to the natural heterogeneity of the soil

and the discrepancy of the data or methods used in the studies (Yu *et al.* 2007; Zhang and Shao 2014).

Field studies of SOC at watershed scales in the hinterland of the QTP, where the average elevation is ca. 4500 m a.s.l., however, are comparatively rare. Understanding the spatial distributions and influencing factors of SOC is necessary for managing degraded meadows and for forecasting the impact of climate change on SOC (Yang *et al.* 2016). The verification of large-scale inversion further forces the necessity of field studies in the harsh hinterlands of the QTP.

A dataset for SOC, vegetation coverage (VC) and soil properties was compiled for an alpine meadow to analyze the distribution, stock, and influencing factors of SOC. The specific objectives were to: (1) estimate the total SOC stock and analyze the spatial distribution of the density of soil organic carbon (SOCD) in the study plot, (2) determine the main factors influencing SOCD and evaluate the accuracy of multiple linear regression equation for estimating SOCD.

## 2. Materials and methods

### 2.1 Site description

The study area is in the hinterland of the QTP, in Nagqu prefecture of the Tibet Autonomous Region. The area has an elevation of ca. 4600 m a.s.l. and has a subfrigid climate with long cold winters and short growing seasons (June–August). The annual mean temperature for 1981–2014 varied from  $-2.4$  to  $0.9^{\circ}\text{C}$ , with a mean of  $-0.5^{\circ}\text{C}$ , and the annual mean rainfall varied from 307.5 to 620.5 mm, with a mean of 455.8 mm, 63.7% of which fell from June to August (Nagqu Weather Station). The evapotranspiration was ca. 1800 mm, and the relative humidity was only 53%. The study plot was established in 2011 in a degraded meadow, ca. 19 km north of the Nagqu prefecture. The plot has a width of ca. 480 m from southwest to northeast, a length of 530–770 m from southeast to northwest, and a total area of ca. 33.5 hm<sup>2</sup>. The plot is flat and open and slopes from northwest to southeast with a maximum relative elevation (RE) of ca. 10 m (Zhang *et al.* 2015b). Vegetation in the study area is typical zonal grass dominated by *Kobresia pygmaea* and associated with *Potentilla bifurca*, *Potentilla saundersiana*, *Leontopodium pusillum* and *Carex moorcroftii*, which were all annual herbs. The soil

is typical of alpine meadows with a sand content of ca. 69.4% (Zhu *et al.* 2016) and is classified as sandy loam or sandy clay loam according to world reference base. The soil is shallow in the study area with a maximum depth of about 50 cm. The 0–15 cm layer, known as the mattice pipedon (Yang *et al.* 2016), is compacted with dense roots. The 15–30 cm layer has fewer roots and some gravel and stones, and the 30–50 cm layer has very few roots but some gravel and stones. Stones are distributed extensively below 50 cm, which limited the depth to which soil profiles could be exposed.

## 2.2 Sampling design and data acquisition

We dug 23 pits in the 2015 growing season to access soil profiles. The pits were arranged in a 120 m (southeast to northwest) × 150 m (southwest to northeast) grid and were identified as L1–L23. Eighteen of the 23 pits could be dug to a depth of 50 cm, four of the pits (L1, L3, L8 and L9) were 40 cm in depth, and one (L4) was 20 cm in depth due to the obstruction of stones. Undisturbed and disturbed soil samples were collected at intervals of 10 cm from all profiles using cutting rings with volumes of 100 cm<sup>3</sup> (5 cm in diameter and in height) and zip-lock bags of size eight, respectively. Some undisturbed samples were damaged during transport, leaving 83 undisturbed and 108 disturbed soil samples for analysis.

The undisturbed soil samples were used to measure soil bulk density (*BD*, g cm<sup>-3</sup>), volumetric soil-water content (SWC, %), total porosity (*TP*, %), and saturated hydraulic conductivity (*K<sub>s</sub>*, mm min<sup>-1</sup>) by: (1) weighing the undisturbed natural soil and cutting ring using an electronic balance (*m<sub>ns+cr</sub>*, g), (2) transferring the samples to a vessel, containing water at a level consistent with the upper layer of the cutting ring, (3) removing and weighing the samples after 6 h (*m<sub>ns+cr+6</sub>*, g), (4) drying the samples in an oven at a constant temperature of 105°C for 12 h, and (5) weighing the dry soil and cutting ring (*m<sub>ds+cr</sub>*, g). The *BD*, volumetric SWC, and *TP* were calculated as (Wang and Shao 2013):

$$BD = \frac{m_{ds+cr} - m_{cr}}{V} \quad (1)$$

$$\theta_v = \frac{m_{ns+cr} - m_{ds+cr}}{V} \times BD \times 100\% \quad (2)$$

$$TP = \frac{m_{ns+cr+6} - m_{ds+cr}}{V} \times 100\% \quad (3)$$

where *m<sub>cr</sub>* is the weight of the cutting ring (g), *V* is the volume of the cutting ring (cm<sup>3</sup>), and *θ<sub>v</sub>* is the volumetric SWC (%).

The constant hydraulic head method was used to measure *K<sub>s</sub>*. The undisturbed sample before step (4) above was connected to a Markov bottle to maintain a stable hydraulic head. The outflow was recorded every 10 min until the flow was stable. *K<sub>s</sub>* was calculated as (Wang and Shao 2013)

$$K_s = \frac{10 \cdot Q \cdot L}{A \cdot t \cdot H} \quad (4)$$

where *Q* is the outflow of water (cm<sup>3</sup>), *L* is the length of the flow path (cm), *A* is the cross-sectional area of the flow path (cm<sup>2</sup>), *t* is the flow duration (10 min in this study), and *H* is the hydraulic head (cm).

The disturbed soil samples were weighed after natural drying (*m<sub>nd</sub>*, g), and the samples were then passed through a 2-mm mesh and the coarse particles (>2 mm) were weighed (*m<sub>gs</sub>*, g). Soil gravel and stone content (*SSC*, %) was then calculated as

$$SSC = \frac{m_{gs}}{m_{nd}} \times 100\%. \quad (5)$$

The particles from the disturbed soil samples that passed through the 2-mm mesh were divided into two parts; one was used to measure soil texture using a laser particle sizer (Mastersizer 2000, Malvern Instruments, Britain). Soil texture was described with clay (< 0.002 mm), silt (0.02–0.002 mm), and sand (0.02–2 mm) according to the international taxonomy system. The other part was passed through a 0.25 mm mesh for measuring SOC using the potassium-dichromate external-heating method and soil pH using a pH meter (Mettler Toledo Co., Ltd, Switzerland).

A hand-held GPS receiver was used to record the longitude, latitude, and altitude. The *RE* of the lowest point, L4, was set to 0, and the *REs* of the other points were calculated by subtracting the absolute elevation of L4 (4595 m) from their elevations.

In addition, two photographs were taken at each sampling point by a digital camera (Canon 600D) 0.5 m east and west of the point and 1.2 m above the ground. Photographs of the vegetation at the 23 locations were acquired each week. The VC was determined from the photographs using Image J software, and the mean value was used for analysis.

Table 1. Area of each location.

Plot position	Locations	Length × width (m)	Area (m <sup>2</sup> )
Corner	L1, L4, L23	75 × 60	4500
Edge1	L2, L3, L20	150 × 60	9000
Edge2	L5, L8, L9, L12, L13, L17, L21	120 × 75	9000
Interior	L6, L7, L10, L11, L14–16, L18, L19, L22	150 × 120	18000

Note: Edge1, southeastern and northern edges of the plot; Edge2, southwestern and northeastern edges of the plot.

### 2.3 Calculation of SOCD and SOC stock

$SOCD_{i,j}$  for the  $i$ th layer at location  $j$  ( $SOCD_{i,j}$ , kg m<sup>-2</sup>) was calculated as (Zhang and Shao 2014):

$$SOCD_{i,j} = \frac{SOC_{i,j} \times BD_{i,j} \times D \times (1 - CF_{i,j}/100)}{100} \quad (6)$$

where  $SOC_{i,j}$  is the SOC in the  $i$ th layer at location  $j$  (g kg<sup>-1</sup>),  $BD_{i,j}$  is bulk density in the  $i$ th layer at location  $j$  (g cm<sup>-3</sup>),  $D$  is the thickness of the soil layers (10 cm in this study), and  $CF_{i,j}$  is the fraction of coarse fragments >2 mm in the  $i$ th layer at location  $j$  (%).

The SOC stock was calculated as:

$$SOC_{i,stock} = \sum_{j=1}^m (SOCD_{i,j} \times S_j) \quad (7)$$

where  $SOC_{i,stock}$  is the amount of SOC in the  $i$ th layer of the plot (kg),  $m$  is the number of sampling locations ( $m = 23$  in this study), and  $S_j$  is the area location  $j$  represents. Because the sampling points were at different locations in the plot, the areas the sampling points can represent differed (table 1).

The amount of SOC ( $SOC_{stock}$ , kg) for the entire plot was thus calculated as:

$$SOC_{stock} = \sum_{i=1}^n SOC_{i,stock} \quad (8)$$

where  $n$  is the number of soil layers ( $n = 5$  in this study).

### 2.4 Statistics and evaluation

Classical statistical methods were used to analyze the spatial variation of SOCD following the steps: (1) describe and exhibit the statistical parameters of maximum, minimum, mean, median, range, standard deviation (SD), coefficient of variation

(CV); (2) determine the type of distribution of the variables; and (3) judge the degree of the variation of the samples based on the CV, which is the ratio of SD and the mean. Variation is generally considered to be low, moderate, and high at  $CV \leq 10\%$ ,  $10\% < CV < 100\%$ , and  $CV \geq 100\%$ , respectively (Nielsen and Bouma 1985).

A one-way analysis of variance (ANOVA) was used to analyze the differences in SOCD in the various soil layers. Pearson correlation coefficients were used to determine the correlations between SOCD and its influencing factors. Single sample K-S testing was used to test the distribution of SOCD.

Multiple linear regression was used to estimate SOCD. Odd numbered samples were used to build the regression equation, and even numbered samples were used to evaluate the model. The root mean square error ( $RMSE$ ) and the Nash–Sutcliffe model efficiency coefficient ( $NSE$ ) (Nash and Sutcliffe 1970) were used to evaluate the accuracy of the model

$$RMSE = \sqrt{\frac{1}{N} \sum_{i=1}^N (SOCD_m - SOCD_s)^2} \quad (9)$$

where  $N$  is the number of soil samples that used to build the model;  $SOCD_m$  is the measured SOCD (kg m<sup>-2</sup>) and  $SOCD_s$  is the simulated SOCD (kg m<sup>-2</sup>).

$$NSE = 1 - \frac{\sum_{i=1}^N (SOCD_{m,i} - SOCD_{s,i})^2}{\sum_{i=1}^N (SOCD_{m,i} - \overline{SOCD_{m,i}})^2} \quad (10)$$

$NSE$  ranges from  $-\infty$  to 1.  $NSE = 1$  indicates that the simulated and measured SOCD are the same;  $NSE = 0$  indicates that the estimate is as accurate as the mean measured SOCD; and an  $NSE < 0$  indicates that the simulated SOCD is not as accurate as the mean measured SOCD (Nash and Sutcliffe 1970; Yuan et al. 2016).

### 3. Results and discussion

#### 3.1 Descriptive statistics of the soil physical properties

Soil physical properties are important factors influencing SOC, so describing the basic properties of the soil in a study area is necessary. The mean values of  $K_s$ ,  $BD$ ,  $TP$ , clay, silt and sand contents, and  $SSC$  were  $2.02 \text{ mm min}^{-1}$ ,  $1.37 \text{ g cm}^{-3}$ ,

$28.24$ ,  $16.82$ ,  $13.75$ ,  $69.40$  and  $40.61\%$ , respectively (table 2). The  $K_s$  varied more spatially, and the other properties varied moderately.  $BD$  and  $SSC$  in the profiles increased with depth;  $TP$ , silt content, and  $SWC$  decreased with depth; and  $K_s$ , clay and sand contents did not vary with depth. The amounts of roots decreased and gravel increased with depth, which may have increased  $BD$  and decreased  $TP$  with depth. The study area suffered

Table 2. Descriptive statistics for the primary soil properties.

Property	Layer (cm)	Maximum	Minimum	Mean	SD	CV (%)
$K_s$ ( $\text{mm min}^{-1}$ )	0–10	5.88	0.10	1.53	1.55	101.34
	10–20	9.79	0.20	3.19	2.49	78.19
	20–30	6.15	0.03	1.78	2.11	118.58
	30–40	4.83	0.18	1.82	1.62	89.00
	40–50	6.21	0.02	1.78	1.81	101.79
$BD$ ( $\text{g cm}^{-3}$ )	0–10	1.69	0.71	1.04	0.22	21.28
	10–20	1.69	1.07	1.42	0.17	12.04
	20–30	1.66	1.03	1.43	0.18	12.88
	30–40	1.75	1.27	1.53	0.12	8.06
	40–50	1.79	1.32	1.61	0.14	8.84
$TP$ (%)	0–10	48.01	17.62	30.53	8.35	27.36
	10–20	39.93	24.58	30.93	4.72	15.27
	20–30	34.80	18.43	27.30	4.55	16.65
	30–40	40.96	14.57	25.96	6.60	25.42
	40–50	32.90	19.30	24.74	3.66	14.77
Clay content (%)	0–10	23.41	13.08	17.77	2.58	14.52
	10–20	22.90	2.53	14.58	4.65	31.86
	20–30	39.15	9.11	16.99	6.56	38.62
	30–40	27.41	8.19	17.58	4.77	27.13
	40–50	25.44	6.36	17.31	4.86	28.08
Silt content (%)	0–10	19.98	11.47	16.16	2.24	13.86
	10–20	19.77	2.78	13.30	4.03	30.30
	20–30	25.11	7.93	13.44	3.76	27.95
	30–40	18.88	4.72	13.02	3.44	26.44
	40–50	18.32	6.91	12.49	3.40	27.20
Sand content (%)	0–10	73.65	57.91	66.07	4.56	6.90
	10–20	94.69	57.40	72.12	8.45	11.71
	20–30	80.63	35.74	69.55	9.93	14.28
	30–40	87.09	54.58	69.33	7.74	11.17
	40–50	86.73	56.24	70.09	7.50	10.70
Soil gravel and stone content (%)	0–10	45.07	4.78	27.65	12.09	43.74
	10–20	57.39	8.75	38.95	9.60	24.64
	20–30	60.87	33.94	43.83	7.57	17.26
	30–40	58.49	25.83	45.31	10.49	23.15
	40–50	64.95	26.74	49.35	10.67	21.63
Soil-water content (%)	0–10	38.43	4.23	21.87	10.85	49.59
	10–20	23.67	1.79	9.29	5.79	62.40
	20–30	11.91	1.89	7.24	2.83	39.03
	30–40	14.44	1.53	6.43	3.49	54.19
	40–50	7.36	1.93	4.62	1.77	38.25

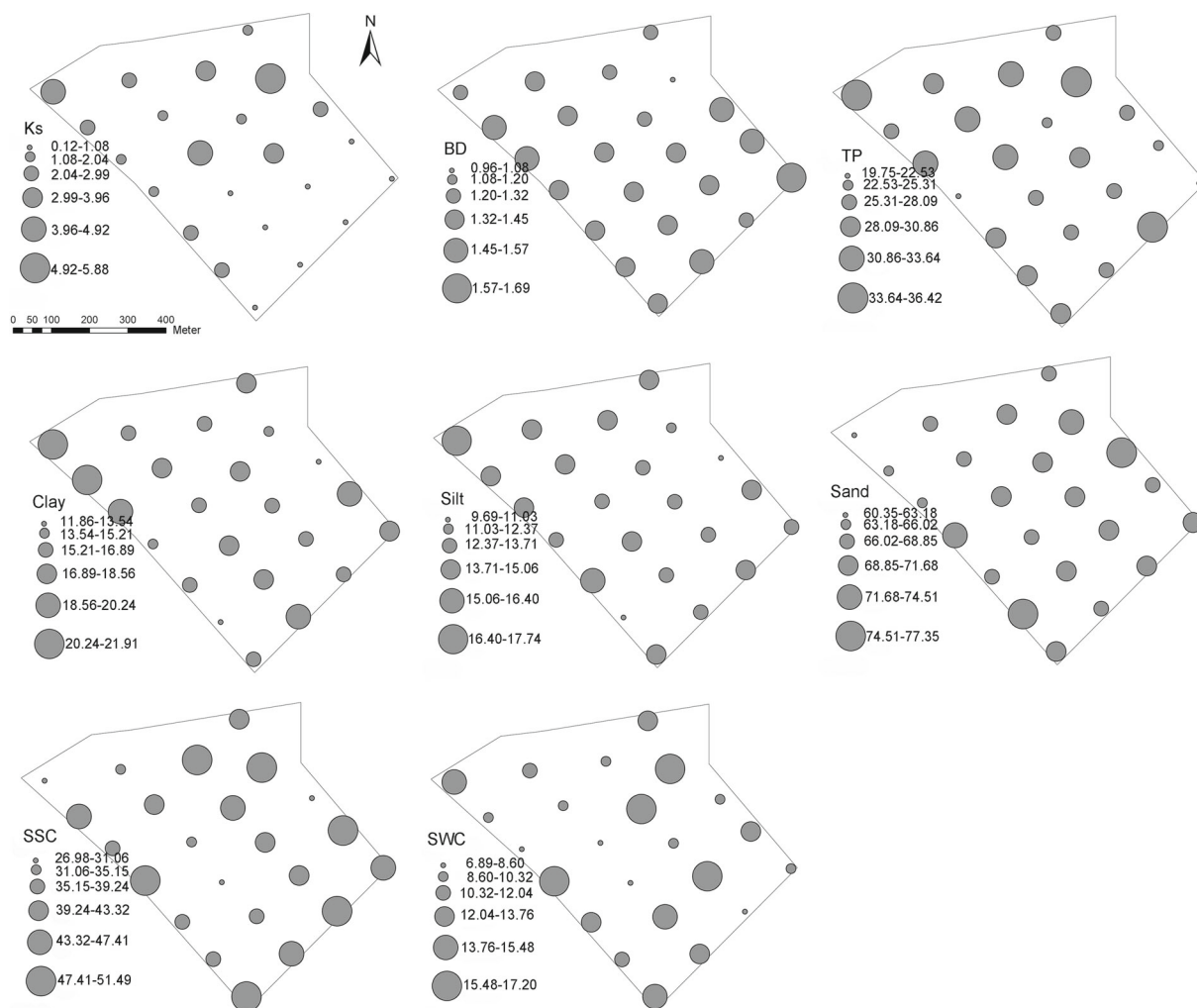


Figure 1. Horizontal distribution of the mean values of soil saturated hydraulic conductivity ( $K_s$ , mm min<sup>-1</sup>); bulk density ( $BD$ , g cm<sup>-3</sup>); total porosity ( $TP$ , %); soil clay, silt, and sand contents (%); soil gravel and stone content ( $SSC$ , %), and soil-water content ( $SWC$ , %).

a drought in July 2015, so  $SWC$  had not recovered throughout the profile, although some rain fell in August, which may account for the decrease in  $SWC$  with depth.

The  $K_s$  was high in the central and northwestern parts of the plot,  $BD$  was lower in the north, and  $TP$  was low in the central and eastern parts of the plot (figure 1). The distributions of clay, silt, and sand contents were similar; all were low in the northeast and southwest.  $SSC$  was higher in the northern and southeastern parts of the plot.  $SWC$  did not vary. The soil in the northwest of the plot generally had high  $K_s$  and  $TP$  and low  $BD$  and  $SSC$ , which were suitable for  $SWC$ , nutrient migration, and vegetation growth. The distribution of the soil properties may have been due to the  $RE$ , although the largest  $RE$  was only 10 m; the terrain was higher in the northwest and lower in the

southeast, which may have caused the variations in the soil properties (Leifeld *et al.* 2005; Chen *et al.* 2016; Xin *et al.* 2016).

## 3.2 Statistics and distribution of SOCD

### 3.2.1 Statistical analysis of SOCD

Mean SOCD in our study plot was 2.28 kg m<sup>-2</sup> to a depth of 50 cm, with a range of 5.99 kg m<sup>-2</sup> (table 3). The single-sample K-S test ( $p < 0.05$ ) indicated an abnormal distribution. The distance from the median to the maximum was 3.8 times the distance from the median to the minimum, indicating a right-skewed distribution. The SD of SOCD was 1.42, and the CV was 62.19%, indicating a moderately variable SOCD. Mean SOCD decreased

Table 3. Descriptive statistics for the density of soil organic carbon (SOCD,  $\text{kg m}^{-2}$ ) and the SOC stocks (kg) in the soil layers of the study plot.

Layer (cm)	N	Maximum	Minimum	Mean	Median	Range	SD	CV (%)	SOC stock (kg)	Proportion (%)
0–10	22	6.17	2.54	3.94	3.95	3.63	0.78	19.95	1116.30	37.9
10–20	17	6.54	1.58	2.86	2.52	4.96	1.23	43.05	800.74	27.1
20–30	13	2.53	0.91	1.55	1.45	1.63	0.48	31.26	437.19	14.8
30–40	15	2.84	0.55	1.15	1.02	2.29	0.58	50.21	319.35	10.8
40–50	15	1.33	0.81	0.97	0.88	0.52	0.17	17.92	276.38	9.4
0–50	82	6.54	0.55	2.28	1.79	5.99	1.42	62.19	2949.95	100

Note: N: sample size; SD: standard deviation; CV: coefficient of variation.

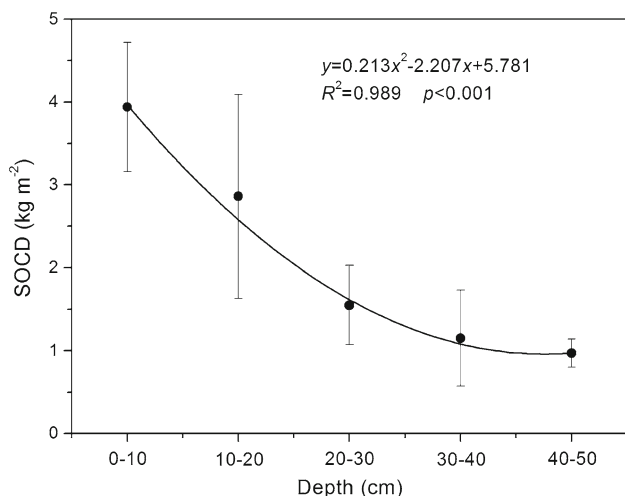


Figure 2. Fitted curve for the vertical distribution of the density of soil organic carbon (SOCD,  $\text{kg m}^{-2}$ ). Vertical bars correspond to  $\pm 1$  standard deviation of the SOCD.

with depth, mainly due to the decrease in the number of roots and to the increase in *SSC* (table 2). One-way ANOVA analysis showed that the difference between the mean SOCD in the five layers was significant at  $p < 0.001$ . The stock of SOC in the plot was ca. 2950 t, with the 0–10 and 0–20 cm layers accounting for 37.8 and 65.0%, respectively. The temperature was low in the study area during the non-growing seasons, and the surface SWC was nearly saturated during the growing seasons in normal years, which decreased the decomposition rates of dead roots and litter and resulted in the accumulation of SOC in the surface layer. Yang *et al.* (2016) reported the same result for the northeastern QTP, where the soil was deeper than in our study area and the mattic epipedon of the 0–14 cm layer accounted for 21% of the SOC in the upper 1 m of soil.

Measures of SOCD have differed in SOC studies on the QTP due to the influences of topography,

vegetation, soil properties, and permafrost distribution. Yang *et al.* (2016) estimated a slightly higher SOCD in a meadow on the northeastern edge of the QTP. Mean SOCD to a depth of 50 cm in another study of meadow ecosystems on the QTP was  $7.51 \text{ kg m}^{-2}$ , which was three times higher than in our study (Yang *et al.* 2008). The altitudes of these studies were lower than in our study area, and another study reported that high altitude can reduce the turnover rate of SOCD (Leifeld *et al.* 2005). The soil in our study area, however, developed shallow, with a mean depth of about 50 cm; *SSC* was high, with a mean of 40.6% to a depth of 50 cm, and the meadow was degraded to some extent and had low VC and above ground biomass (average of  $74 \text{ g m}^{-2}$  for 9 and 27 July and 24 August). The shallow soil, high *SSC*, and the degraded vegetation can account for the lower SOCD, which could obscure the increase in SOCD with altitude in our study area.

### 3.2.2 Vertical pattern of SOCD

SOCD varied specifically within the soil profile, even though the soil was shallow. SOCD decreased quadratically with depth (figure 2). The values of SOCD in the 10, 20, 30, 40, and 50 cm soil layers were  $3.94 \pm 0.78$ ,  $2.86 \pm 1.23$ ,  $1.55 \pm 0.48$ ,  $1.15 \pm 0.58$ , and  $0.97 \pm 0.17 \text{ kg m}^{-2}$ , respectively (table 3). SOCD was higher in the 0–20 cm layers and lower in the 30–50 cm layers, where, however, SD was lower, indicating a relatively homogeneous distribution of SOCD. Studies have reported that SOCD decreased with depth exponentially (Meersmans *et al.* 2009b) or logarithmically (Li and Shao 2014), but SOCD in our study was best described by a quadratic function ( $R^2 = 0.989$ ,  $p < 0.001$ ). The differences may be caused by differences in soil properties, vegetation, and climatic factors.

### 3.2.3 Horizontal variation and distribution of SOCD

SOCD varied moderately spatially, and the degree of variation was not dependent on depth (table 3). SOCD generally varied less in the 0–10 and 40–50 cm than the middle layers. Studies have reported that SOCD in the surface layer was sensitive to vegetation, climate, land-use type and management strategy and varied more than in deeper layers (Li and Shao 2014). The 0–10 cm layer in our study area, however, was the mottic epipedon, where the hardened root-soil structure was conducive to the stocks of SOC and weakened the influence of the external environment. In addition, the 40–50 cm layer lay at the bottom of the profile was weak affected by the vegetation, climate, and human activities.

The distributions of SOCD in the various soil layers were obtained using Kriging interpolation (figure 3). SOCD in the 30–40 cm layer was concentrated in the south of the plot, and SOCD in the 40–50 cm layer was concentrated in the central part. SOCD in the other three soil layers all tended to increase from southeast to northwest, which was consistent with the distribution of  $K_s$ ,  $TP$ , and silt content and in contrast to the distribution of  $BD$  (figure 1), indicating that the soil properties and water conditions were better in the northwestern than the central and southeastern parts of the plot, which may have contributed to the distribution of SOCD.

### 3.3 Factors influencing SOCD

Pearson correlations between SOCD in each layer and the influencing factors were consistent with the correlations between SOCD in the entire profile and the influencing factors, except for some factors in the 0–10 and 40–50 cm layers (table 4). SOCD was significantly correlated positively with  $SWC$ ,  $TP$ , and silt content at  $p < 0.01$  and negatively with  $BD$ ,  $SSC$ , and  $pH$  at  $p < 0.01$  and with sand content at  $p < 0.05$ .

Studies have reported positive correlations between the contents of fine soil particles (silt and clay) and SOCD (Li and Shao 2014; Zhang and Shao 2014). Fine soil particles and iron oxide can fix soil organic matter (Li and Shao 2014), which may mostly account for the positive correlation. In addition, soil porosity can promote the aggregation of SOC to some extent, and  $SWC$  can protect the SOC from oxidization. The increase in

$BD$ ,  $SSC$ , and sand content indicates a decrease in fine particles, so SOC accordingly decreased. The alpine-meadow soil was weakly acidic, with a mean  $pH$  of 6.75 and a range of 5.75–7.51. A small change in  $pH$  can greatly influence the structure and function of microbial communities (Curtin *et al.* 1998), and accordingly influence the content of organic carbon.

The inconsistency of significant differences between the individual layers and the entire profile (0–50 cm) was mainly due to the special features of the area and the number of samples (table 4) for each layer. A comparison between SOCD and the other properties among the layers can provide an indirect understanding of the soil structure. For example, the correlations of the clay, silt, and sand contents with the SOCDs in the 10–20, 20–30, 30–40 and 40–50 cm layers were consistent with the correlations of the clay, silt, and sand contents with the SOCD in the entire profile. SOCD in the 0–10 cm layer, however, was oppositely correlated, which may indicate that the features of the 0–10 cm layer are distinct from those of the other layers and that the mottic epipedon has an important influence on the soil properties in return. Samples of the entire soil profile can generally represent the overall condition of the soil and can be used for regression analysis.

### 3.4 Simulation and estimation of SOCD

The Pearson analysis showed that  $SWC$ ,  $BD$ ,  $TP$ , silt content,  $SSC$ , and  $pH$  were all significantly correlated with SOCD. To avoid the influence of collinearity of the factors, we chose  $BD$ , which was most highly correlated with SOCD, for estimating SOCD.  $pH$ ,  $RE$ , and  $VC$  were then chosen for representing soil chemistry, terrain, and vegetation, respectively.

The regression parameters and efficiencies of the multiple regression equations of each layer are shown in table 5. The models were better for the 0–10 and 20–30 cm layers, with higher  $R^2$  and lower  $p$  values. The model for all samples (0–50 cm) had the best efficiency ( $p < 0.001$ ), with the highest  $R^2$  of 0.656.

Cross validation was used to verify the multiple regression equation. Data from the odd numbered rows were chosen to build the regression equation for SOCD, and the even numbered rows were used to evaluate the performance of the equation. The equation was



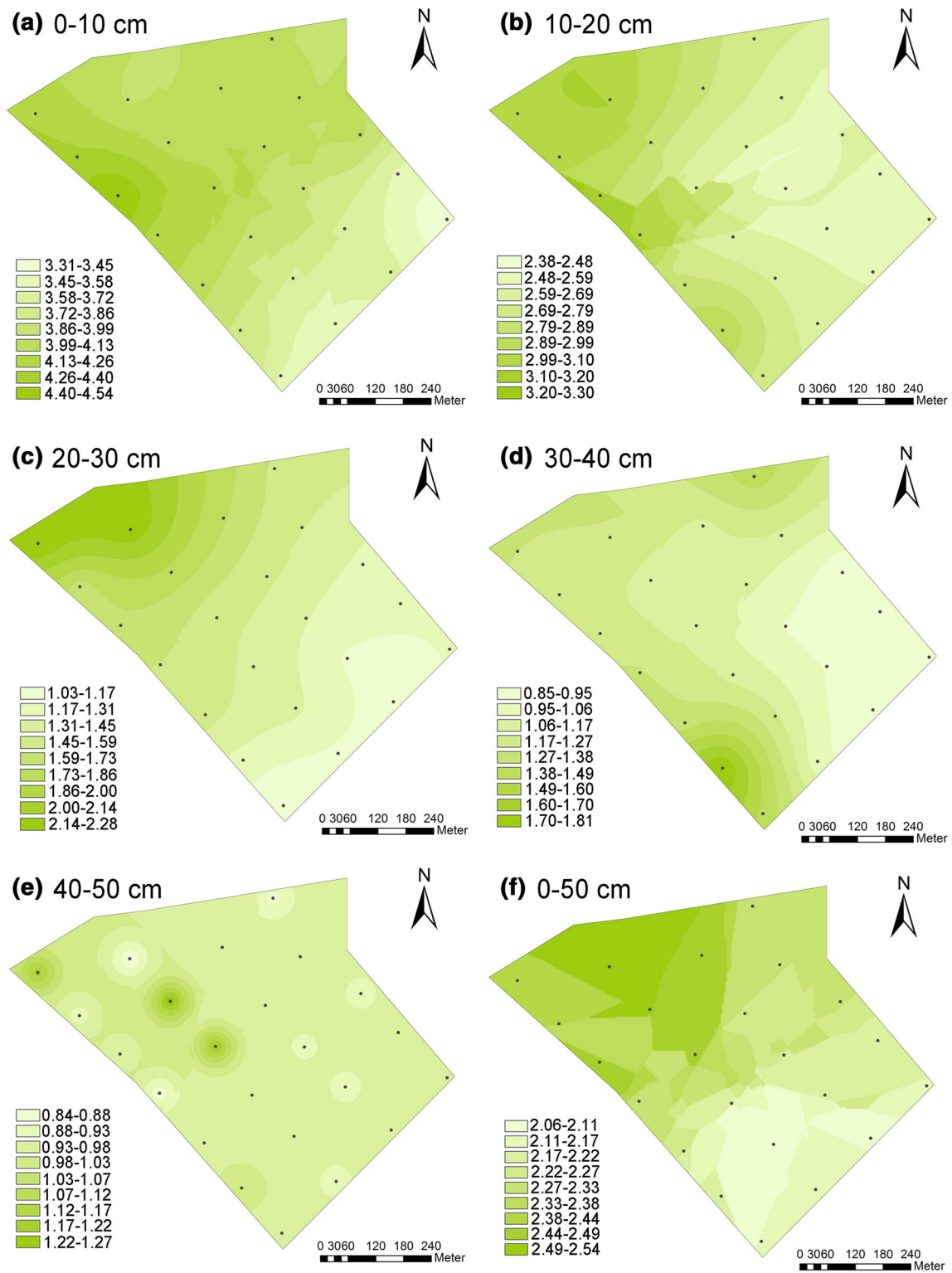


Figure 3. Spatial distribution of the density of soil organic carbon (SOCD,  $\text{kg m}^{-2}$ ) in the various soil layers.

$$\begin{aligned}
 \text{SOCD} = & -0.035 * RE - 1.514 * BD - 2.215 * pH \\
 & -0.501 * VC + 19.366 \\
 (N = 41, R^2 = 0.547, p < 0.001). \quad (11)
 \end{aligned}$$

The measured SOCD was plotted against the estimated SOCD to test the utility of the equation (figure 4). All points were near the 1:1 line, the correlation coefficient and *NSE* were high, and

Table 4. Pearson correlation coefficients between the density of soil organic carbon and environmental factors in the soil layers.

Layer (cm)	RE	SWC	$K_s$	BD	TP	Clay content	Silt content	Sand content	SSC	pH	VC
0–10	0.372	-0.336	0.175	-0.282	0.660**	-0.145	-0.051	0.108	-0.414	-0.433*	0.694**
10–20	0.362	0.134	-0.004	-0.123	-0.212	0.298	0.354	-0.329	-0.320	-0.395	0.088
20–30	0.731**	0.075	0.754**	-0.074	0.197	0.025	0.197	-0.089	-0.713**	-0.418	0.134
30–40	0.228	0.755**	-0.007	-0.464	0.002	0.166	0.288	-0.235	-0.123	-0.065	0.117
40–50	0.148	-0.039	0.086	0.119	0.362	0.419	0.514	-0.503	-0.391	0.204	0.466
0–50	0.155	0.547**	0.094	-0.674**	0.414**	0.062	0.412**	-0.231*	-0.646**	-0.785**	0.112

Note: RE: relative elevation (m); SWC: soil–water content ( $\text{cm}^3 \text{cm}^{-3}$ );  $K_s$ : saturated hydraulic conductivity ( $\text{mm min}^{-1}$ ); BD: soil bulk density ( $\text{g cm}^{-3}$ ); TP: total porosity (%); VC: vegetation coverage.

\*indicates the correlation is significant at  $p < 0.05$ ; \*\*indicates the correlation is significant at  $p < 0.01$

Table 5. Multiple linear regression analysis of soil organic carbon density in various soil layers.

Layer (cm)	N	Regression parameter					$R^2$	$p$
		RE	BD	pH	VC	constant		
0–10	22	0.072	1.025	-0.382	3.724	2.356	0.567	0.005
10–20	17	0.088	0.228	-2.354	0.055	17.104	0.188	0.609
20–30	13	0.100	-0.499	-1.040	0.302	8.371	0.613	0.077
30–40	15	0.053	-2.040	0.585	0.389	-0.203	0.258	0.515
40–50	15	0.012	0.213	0.312	0.767	-2.161	0.392	0.247
0–50	82	0.015	-1.401	-2.263	-0.295	19.158	0.656	0.000

Note. N: sample size; RE: relative elevation (m); BD: soil bulk density ( $\text{g cm}^{-3}$ ); VC: vegetation coverage.

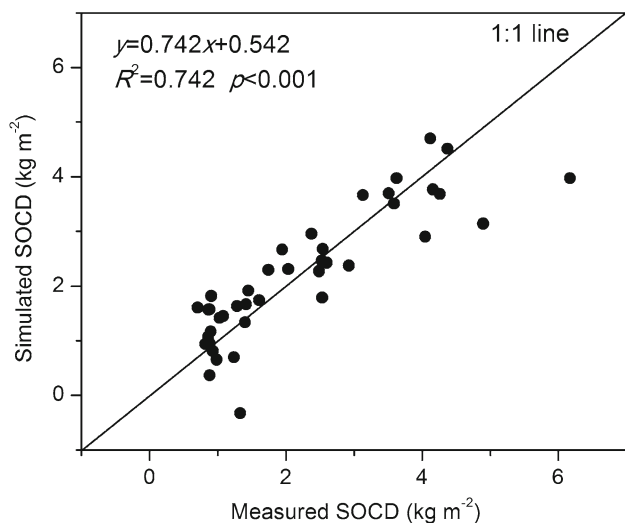


Figure 4. Comparison of measured and simulated densities of soil organic carbon (SOCD).

the estimation error was small ( $\text{RMSE} = 0.692 \text{ kg m}^{-2}$ ). These results indicated that estimating SOCD in the alpine meadow soil using RE, BD, pH, and VC can be acceptably accurate. The study

area was small relative to the entire QTP, but the present study was meaningful for characterizing the alpine meadows in the hinterland of the QTP, where the soil, vegetation, and climate are similar.

#### 4. Conclusion

We investigated the distribution, stocks, and influencing factors of SOCD in the hinterland of the Qinghai–Tibetan Plateau by digging 23 soil pits in an alpine meadow ecosystem. The mean SOCD was  $2.28 \text{ kg m}^{-2}$  to a depth of 50 cm and was moderately variable. Vertically, SOCD decreased quadratically with depth. The total stock of SOC in the study plot was ca. 2950 t, the 0–10 cm layer accounting for 38% of the total and the 0–30 cm layer for 80%. Horizontally, SOCD was higher in the northwestern and lower in the central and southeastern parts of the study plot, which may have been due to the variation of the soil properties and water conditions. SWC, BD, TP, silt content, sand content, SSC, and pH

were the main factors influencing SOCD. A multiple linear regression equation using *RE*, *BD*, *pH*, and *VC* estimated SOCD with acceptable accuracy.

## Acknowledgements

This study was financially supported by the National Natural Science Foundation of China (No. 41230746). Special thanks goes to Dr Xiaoxu Jia and Dr Laiming Huang for their valuable suggestions and discussions. We are also grateful to Dr Yangjian Zhang, Dr Juntao Zhu, Dr Yaojie Liu, Dr Ning Chen and Junxiang Li for their help in the field work.

## References

- Aitkenhead M J and Coull M C 2016 Mapping soil carbon stocks across Scotland using a neural network model; *Geoderma* **262** 187–198.
- Bameri A, Khormali F, Kiani F and Dehghani A A 2015 Spatial variability of soil organic carbon in different hill-slope positions in Toshan area, Golestan Province, Iran: Geostatistical approaches; *J. Mt. Sci.* **12** 1422–1433.
- Batjes N H 1996 Total carbon and nitrogen in the soils of the world; *Eur. J. Soil Sci.* **47** 151–163.
- Baumann F, He J S, Schmidt K, Kühn P and Scholten T 2009 Pedogenesis, permafrost, and soil moisture as controlling factors for soil nitrogen and carbon contents across the Tibetan Plateau; *Glob. Change Biol.* **15** 3001–3017.
- Chen L F, He Z B, Du J, Yang J J and Zhu X 2016 Patterns and environmental controls of soil organic carbon and total nitrogen in alpine ecosystems of northwestern China; *Catena* **137** 37–43.
- Curtin D, Campbell C A and Jalil A 1998 Effects of acidity on mineralization: pH-dependence of organic matter mineralization in weakly acidic soils; *Soil Biol. Biochem.* **1** 57–64.
- Fu X L, Shao M A, Wei X R and Horton R 2010 Soil organic carbon and total nitrogen as affected by vegetation types in Northern Loess Plateau of China; *Geoderma* **155** 31–35.
- He S Y and Richards K 2015 Impact of meadow degradation on soil water status and pasture management – a case study in Tibet; *Land Degrad. Dev.* **26** 468–479.
- Koszinski S, Miller B A, Hierold W, Haelbich H and Sommer M 2015 Spatial modeling of organic carbon in degraded peatland soils of northeast Germany; *Soil Sci. Soc. Am. J.* **79** 1496–1508.
- Leifeld J, Bassin S and Fuhrer J 2005 Carbon stocks in Swiss agricultural soils predicted by land-use, soil characteristics, and altitude; *Agric. Ecosyst. Environ.* **105** 255–266.
- Li D F and Shao M A 2014 Soil organic carbon and influencing factors in different landscapes in an arid region of northwestern China; *Catena* **116** 95–104.
- Li X L, Gao J, Brierley G, Qiao Y M, Zhang J and Yang Y W 2014 Rangeland degradation on the Qinghai–Tibetan Plateau: Implications for rehabilitation; *Land Degrad. Dev.* **24** 72–80.
- Li W J, Li J H, Liu S S, Zhang R L, Qi W, Zhang R Y, Knops J M H and Lu J F 2016 Magnitude of species diversity effect on aboveground plant biomass increases through successional time of abandoned farmlands on the eastern Tibetan Plateau of China; *Land Degrad. Dev.* **27** 370–378.
- Liu Z P, Shao M A and Wang Y Q 2011 Effect of environmental factors on regional soil organic carbon stocks across the Loess Plateau region, China; *Agric. Ecosyst. Environ.* **142** 184–194.
- Meersmans J, van Wesemael B, de Ridder F, Dotti M F, de Baets S and van Molle M 2009a Changes in organic carbon distribution with depth in agricultural soils in northern Belgium, 1960–2006; *Glob. Change Biol.* **15** 2739–2750.
- Meersmans J, van Wesemael B, De Ridder F and van Molle M 2009b Modelling the three-dimensional spatial distribution of soil organic carbon (SOC) at the regional scale (Flanders, Belgium); *Geoderma* **152** 43–52.
- Mulder V L, Lacoste M, Richer-de-Forges A C, Martin M P and Arrouays D 2016 National versus global modelling the 3D distribution of soil organic carbon in mainland France; *Geoderma* **263** 16–34.
- Nash J E and Sutcliffe J V 1970 River flow forecasting through conceptual models. Part 1. A discussion of principle; *J. Hydrol.* **10** 282–290.
- Nielsen D R and Bouma J 1985 *Soil spatial variability*; Pudoc, Wageningen.
- Otto S, Beckers V, Jacxsens P, Hermy M and van Orshoven J 2015 Multi-level statistical soil profiles for assessing regional soil organic carbon stocks; *Geoderma* **253** 12–20.
- Qiu J 2008 The third pole; *Nature* **454** 393–396.
- Ricker M C and Lockaby B G 2015 Soil organic carbon stocks in a large eutrophic floodplain forest of the southeastern atlantic coastal plain, USA; *Wetlands* **35** 291–301.
- Roßkopf N, Fell H and Zeitz J 2015 Organic soils in Germany, their distribution and carbon stocks; *Catena* **133** 157–170.
- Rodríguez Martín J A, Álvaro-Fuentes J, Gonzalo J, Gil C, Ramos-Miras J J, Grau Corbí J M and Boluda R 2016 Assessment of the soil organic carbon stock in Spain; *Geoderma* **264** 117–125.
- Shi Y, Baumann F, Ma Y, Song C, Kühn P, Scholten T and He J S 2012 Organic and inorganic carbon in the topsoil of the Mongolian and Tibetan grasslands: pattern, control and implications; *Biogeosci.* **9** 2287–2299.
- Sun H L, Zheng D, Yao T D and Zhang Y L 2012 Protection and construction of the national ecological security shelter zone on Tibetan Plateau; *J. Geogr. Sci.* **67** 3–12 (in Chinese with English abstract).
- Tan K, Ciais P, Piao S L, Wu X P, Tang Y H, Vuichard N, Liang S and Fang J Y 2010 Application of the ORCHIDEE global vegetation model to evaluate biomass and soil carbon stocks of Qinghai–Tibetan grasslands; *Glob. Biogeochem. Cycle.* **24**, <https://doi.org/10.1029/2009GB003530>.
- Wang G X, Qian J, Cheng G D and Lai Y M 2002 Soil organic carbon pool of grassland soils on the Qinghai–Tibetan Plateau and its global implication; *Sci. Total Environ.* **291** 207–217.

- Wang G C, Huang Y, Zhang W, Yu Y Q and Sun W J 2015a Quantifying carbon input for targeted soil organic carbon sequestration in China's croplands; *Plant Soil* **394** 57–71.
- Wang J M, Yang R X and Bai Z K 2015b Spatial variability and sampling optimization of soil organic carbon and total nitrogen for Minesoils of the Loess Plateau using geostatistics; *Ecol. Eng.* **82** 159–164.
- Wang Y Q and Shao M A 2013 Spatial variability of soil physical properties in a region of the Loess Plateau of PR China subject to wind and water erosion; *Land Degrad. Dev.* **24** 296–304.
- Wei X R, Shao M A, Fu X L and Horton R 2010 Changes in soil organic carbon and total nitrogen after 28 years grassland afforestation: Effects of tree species, slope position, and soil order; *Plant Soil* **331** 165–179.
- Wen D and He N P 2016 Forest carbon storage along the north-south transect of eastern China: Spatial patterns, allocation, and influencing factors; *Ecol. Indic.* **61** 960–967.
- Xin Z B, Qin Y B and Yu X X 2016 Spatial variability in soil organic carbon and its influencing factors in a hilly watershed of the Loess Plateau, China; *Catena* **137** 660–669.
- Yang R M, Zhang G L, Yang F, Zhi J J, Yang F, Liu F, Zhao Y G and Li D C 2016 Precise estimation of soil organic carbon stocks in the northeast Tibetan Plateau; *Sci. Rep.* **6**, <https://doi.org/10.1038/srep21842>.
- Yang Y H, Fang J Y, Tang Y H, Ji C J, Zheng C Y, He J S and Zhu B 2008 Storage, patterns and controls of soil organic carbon in the Tibetan grasslands; *Glob. Change Biol.* **14** 1592–1599.
- Yuan G F, Zhu X C, Tang X Z, Yi X B and Du T 2016 A species-specific and spatially-explicit model for estimating vegetation water requirements in desert riparian forest zones; *Water Resour. Manag.* **30** 3915–3933.
- Yu D S, Shi X Z, Wang H J, Sun W X, Chen J M, Liu Q H and Zhao Y C 2007 Regional patterns of soil organic carbon stocks in China; *J. Environ. Manag.* **85** 680–689.
- Zhang P P and Shao M A 2014 Spatial variability and stocks of soil organic carbon in the Gobi Desert of Northwestern China; *PloS One* **9**, <https://doi.org/10.1371/journal.pone.0093584>.
- Zhang M, Huang X J, Chuai X W, Yang H, Lai L and Tan J Z 2015a Impact of land use type conversion on carbon storage in terrestrial ecosystems of China: A spatial-temporal perspective; *Sci. Rep.* **5**, <https://doi.org/10.1038/srep10233>.
- Zhang T, Zhang Y J, Xu M J, Zhu J T, Wimberly M C, Yu G R, Niu S L, Xi Y, Zhang X Z and Wang J S 2015b Light-intensity grazing improves alpine meadow productivity and adaptation to climate change on the Tibetan Plateau; *Sci. Rep.* **5**, <https://doi.org/10.1038/srep15949>.
- Zhang X Z, Yang Y P, Piao S L, Bao W K, Wang S P, Wang G X, Sun H, Luo T X, Zhang Y J, Shi P L, Liang E Y, Shen M G, Wang J S, Gao Q Z, Zhang Y L and Ouyang H 2015c Ecological change on the Tibetan Plateau; *Chin. Sci. Bull.* **60** 3048–3056 (in Chinese).
- Zhao D S, Wu S H, Dai E F, Dai E F and Yin Y H 2015 Effect of climate change on soil organic carbon in Inner Mongolia; *Int. J. Climatol.* **35** 337–347.
- Zhu X C, Shao M A, Zeng C, Jia X X, Huang L M, Zhang Y J and Zhu J T 2016 Application of cosmic-ray neutron sensing to monitor soil water content in an alpine meadow ecosystem on the northern Tibetan Plateau; *J. Hydrol.* **536** 247–254.

Corresponding editor: NAVIN JUYAL